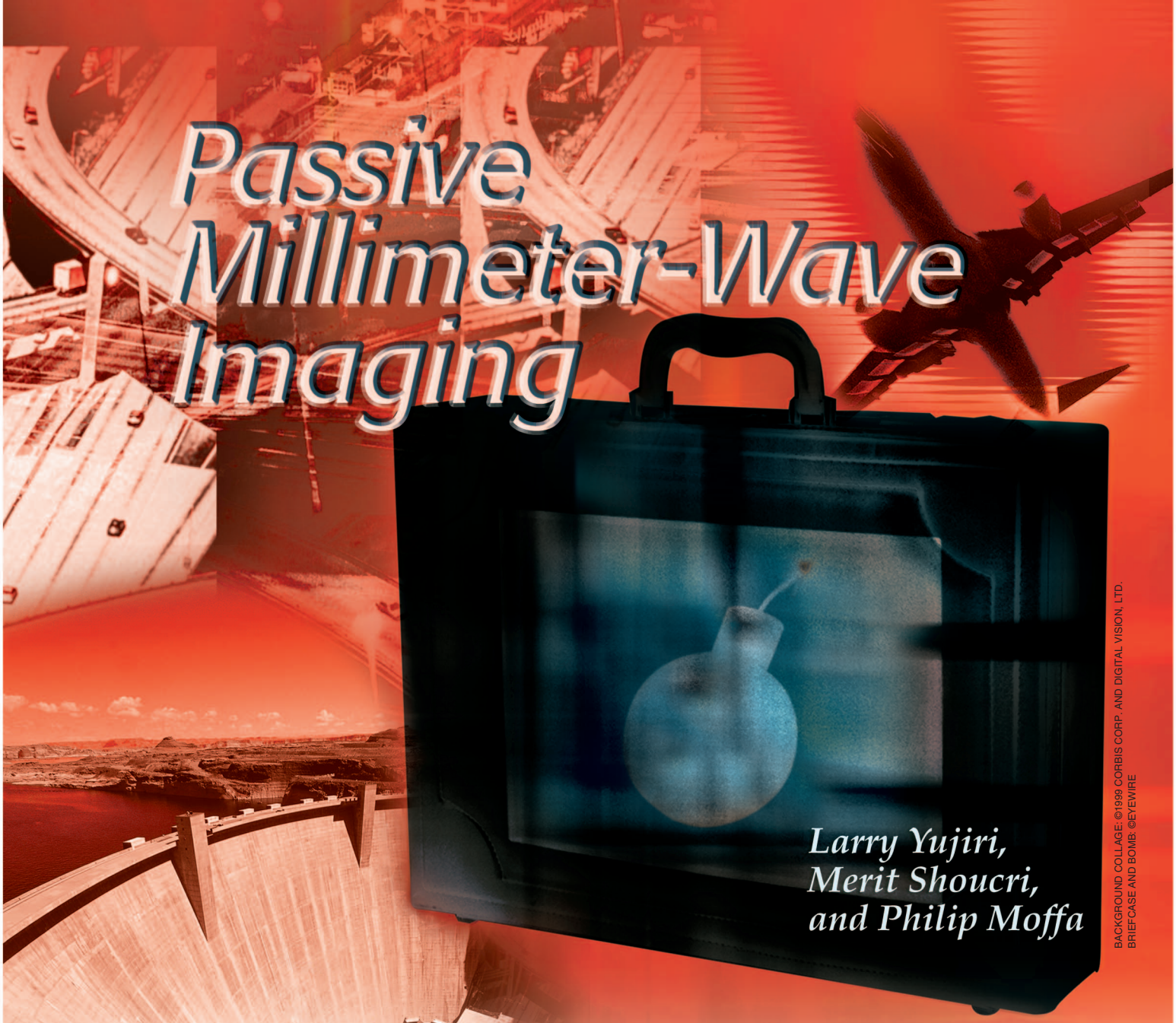
Passive Millimeter-Wave Imaging



Larry Yujiri, Merit Shoucri, and Philip Moffa

BACKGROUND COLLAGE: ©1999 CORBIS CORP. AND DIGITAL VISION, LTD.
BRIEFCASE AND BOMB: ©EYEWIRE

Passive millimeter-wave (PMMW) imaging is a method of forming images through the passive detection of naturally occurring millimeter-wave radiation from a scene. Although such imaging has been performed for decades (or more, if one includes microwave radiometric imaging), new sensor technology in the millimeter-wave regime has enabled the generation of PMMW imaging at video rates and has renewed interest in this area. This interest is, in part, driven by the ability to form images during the day or night; in clear weather or in low-visibility conditions, such as haze, fog, clouds, smoke, or sandstorms; and even through clothing. This ability to see under conditions of low visibility that would ordinarily blind visible or infrared (IR) sensors has the potential to transform the way low-visibility conditions are dealt with. For the military, low visibility can become an asset rather than a liability. In the commercial realm, fog-bound airports could be eliminated as a cause for flight delays or diversions. For security concerns, imaging of concealed weapons could be accomplished in a nonintrusive manner with PMMW imaging.

Like IR and visible sensors, a camera based on PMMW sensors generates easily interpretable imagery in a fully covert manner; no discernible radiation is

Larry Yujiri (larry.yujiri@ngc.com), Merit Shoucri, and Philip Moffa are with Northrop Grumman Space Technology in Redondo Beach, California, USA.

1527-3342/03/$17.00©2003 IEEE

Authorized licensed use limited to: Katholieke Universiteit Leuven. Downloaded on July 02,2010 at 06:43:35 UTC from IEEE Xplore. Restrictions apply.

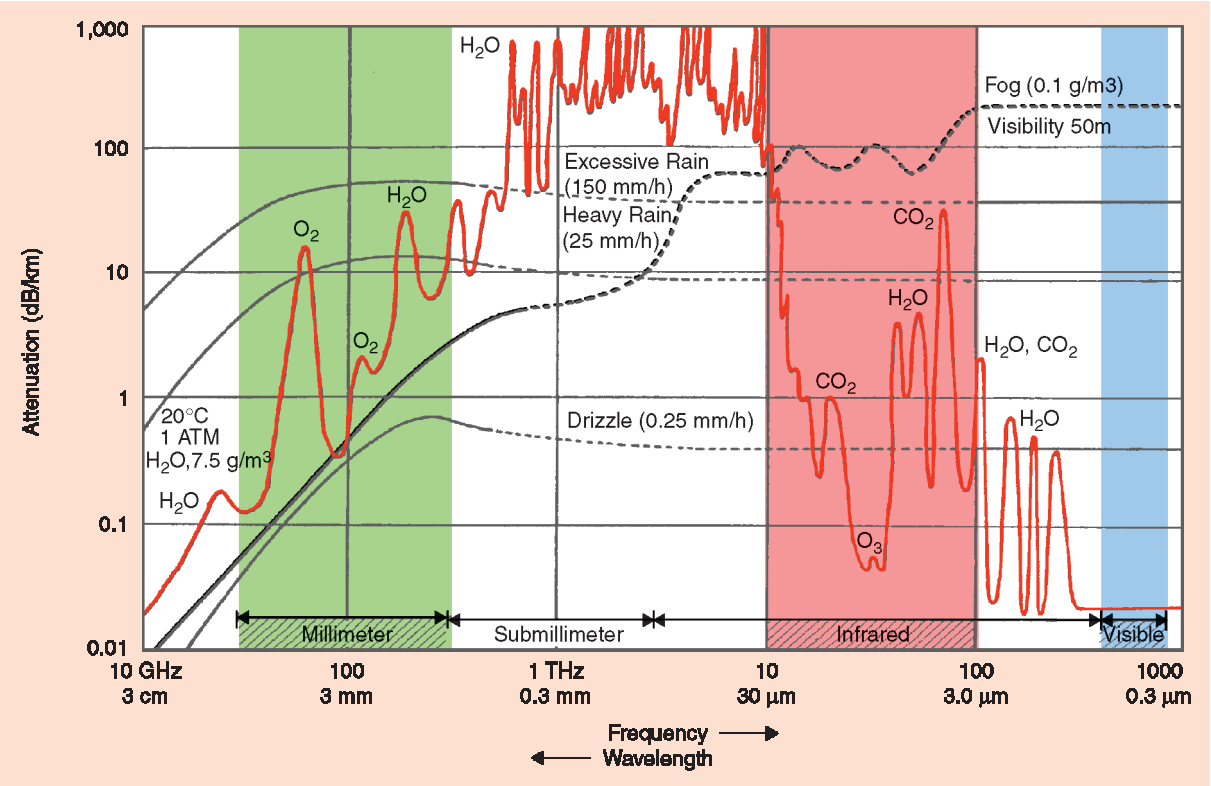


Figure 1. *The attenuation of millimeter waves by atmospheric gases, rain, and fog.*

PMMW imaging has a variety of applications that can be of great use to make life safer and provide the military with a key advantage under low-visibility conditions.

emitted, unlike radar and lidar. However, like radar, PMMW sensors provide penetrability through a variety of low-visibility conditions (moderate/heavy rainfall is an exception). In addition, the underlying phenomenology that governs the formation of PMMW images leads to two important features. First, the signature of metallic objects is very different from natural and other backgrounds. Second, the clutter variability is much less in PMMW images than in other sensor images. Both of these characteristics lead to much easier automated target detection with fewer false alarms.

The wide range of military imaging missions that would benefit from an imaging capability through low-visibility conditions, coupled with its inherent covertness, includes surveillance, precision targeting, navigation, aircraft landing, refueling in clouds, search and rescue, metal detection in a cluttered environment, and harbor navigation/surveillance in fog. Similarly, a number of civilian missions would benefit, such as commercial aircraft landing aid in fog, airport operations in fog, harbor surveillance, highway traffic monitoring in fog, and concealed weapons detection in airports and other locations.

This article introduces the concept of PMMW imaging, describes the phenomenology that defines its performance, explains the technology advances that have made these systems a reality, and presents some of the missions in which these sensors can be used. All of the work presented here has been performed by Northrop Grumman Space Technology (NGST) personnel over the past 15 years and represents a good cross-section of what can be done.

Overview of Millimeter-Wave Radiometry

The regime of the electromagnetic spectrum where it is possible for humans to see is that part where the sun's radiance peaks (at about 6,000 K): the visible regime. In that regime, the human eye responds to different wavelengths of scattered light by seeing different colors. In the absence of sunlight, however, the natural emissions from Earth objects (at about 300 K) are concentrated in the IR regime. Advances in IR-sensor technology in the last 30 years have produced detectors sensitive in that frequency regime, making night vision possible. The exploitation of the millimeter-wave regime (defined to lie between 30 and 300 GHz, with corresponding wavelengths between 10 and 1 mm) follows as a natural progression in the quest to expand our vision. The great advantage of millimeter-wave radiation is that it can be used not only in day and night conditions, but also in

Authorized licensed use limited to: Katholieke Universiteit Leuven. Downloaded on July 02,2010 at 06:43:35 UTC from IEEE Xplore. Restrictions apply.

fog and other poor visibility conditions that normally limit the "seeing" ability of both visual and IR sensors. Many good references exist to introduce imaging in this regime, and a brief overview will be presented here [1]-[3].

Atmospheric Propagation

The usefulness of millimeter waves lies in the peculiarities of atmospheric attenuation phenomenologies over the prescribed frequency range. Figure 1 shows the attenuation of electromagnetic signals in decibels per kilometer of the propagation path length from the microwave through the visible regime [4]. This spans the frequency range from 10 GHz to 1,000 THz, with corresponding free-space wavelengths from 3 cm to 0.3 μm. Propagation of electromagnetic waves over this frequency range is subject to continuum and resonant absorption by various atmospheric constituents, including water in both vapor and droplet form, oxygen, nitrogen, carbon dioxide, ozone, etc. In clear, dry weather, IR and visible radiation propagate with little attenuation; however, atmospheric water content in the form of fog, clouds, and rain causes significant absorption and scattering. In the far IR and submillimeter-wave regime, significant attenuation occurs from water vapor.

Conversely, in the millimeter-wave regime, there are propagation windows at 35, 94, 140, and 220 GHz, where the attenuation is relatively modest in both clear air and fog. Even taking into account the much higher blackbody radiation at IR and visible frequencies, millimeter waves give the strongest signals in fog when propagated over distances of useful interest (see Figure 2). In fact, millimeter-wave radiation is attenuated millions of times less in clouds, fog, smoke, snow, and sandstorms than visual or IR radiation. This is the critical advantage of PMMW imagery. Moreover, millimeter-wave imagery is minimally affected by sun or artificial illumination. Therefore, it operates equivalently in clear or low-visibility conditions during the day or night. It is this ability that makes millimeter waves the best candidate for imaging in most conditions of low visibility.

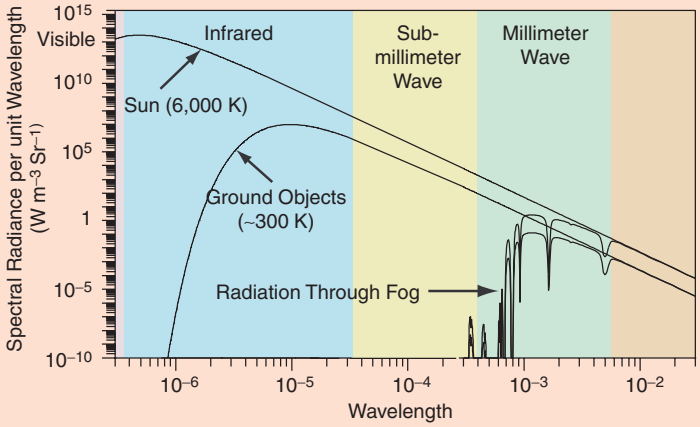


Figure 2. *The effect of fog on the blackbody radiation intensity of the sun (6,000 K) and a ground object (~300 K) as a function of wavelength. Curves are shown for both objects without fog and with the effect of 1 km of fog.*

Table 1. Effective emissivity of common materials at various frequencies.

	Effective Emissivity		
Surface	**44 GHz**	**94 GHz**	**140 GHz**
Bare metal	0.01	0.04	0.06
Painted metal	0.03	0.10	0.12
Painted metal under canvas	0.18	0.24	0.30
Painted metal under camouflage	0.22	0.39	0.46
Dry gravel	0.88	0.92	0.96
Dry asphalt	0.89	0.91	0.94
Dry concrete	0.86	0.91	0.95
Smooth water	0.47	0.59	0.66
Rough or hard-packed dirt	1.00	1.00	1.00

Emissivity and Brightness Temperature

Objects reflect and emit radiation in the millimeter-wave regime, just as they do in the IR and visible regimes. The degree to which an object reflects or emits is characterized by the emissivity (ε) of the object. A perfect radiator (absorber) has $\varepsilon = 1$ and is known as a blackbody. A perfect reflector (nonabsorber) has $\varepsilon = 0$. The emissivity of an object (which is polarization dependent) is a function of the dielectric properties of its constituents, its surface roughness, and the angle of observation. A sampling of emissivities for diverse materials at various frequencies, at normal incidence, and measured at one polarization, is given in Table 1 (based on work performed at NGST.)

When an object's physical thermodynamic temperature T_O is multiplied by its emissivity ε, the resultant product is defined as the object's surface brightness (or radiometric) temperature T_S.

$$T_S = \varepsilon T_O \tag{1}$$

The variation in emissivities of common scene materials, as shown in Table 1, is an important factor in the generation of scene images by causing variations in the power radiated from different parts of the scene. If this were the only factor involved, then images could be

Authorized licensed use limited to: Katholieke Universiteit Leuven. Downloaded on July 02,2010 at 06:43:35 UTC from IEEE Xplore. Restrictions apply.

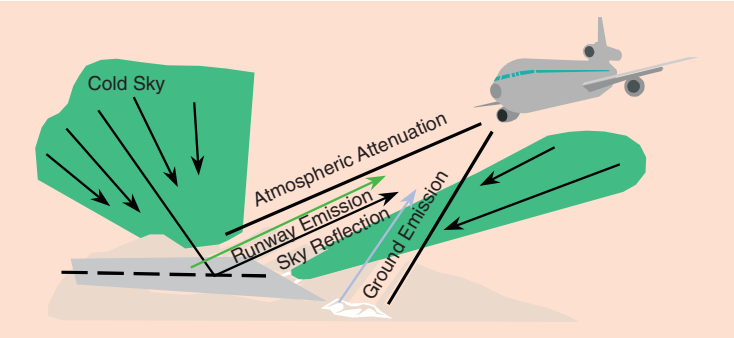


Figure 3. *The observed image is the result of various radiometric effects.*

formed by simply mapping measured values of T_S in the scene. However, the way the scene is illuminated is critical in the way the scene actually looks. For example, a metal plate with $\varepsilon = 0$ will have $T_S = 0$, but, because it is highly reflective, it will appear to have the radiometric temperature of whatever it is reflecting. This effect is captured by a surface scattered radiometric temperature T_{SC} defined as the product of the objects reflectivity ρ and the radiometric temperature $T_{ILLUMINATOR}$ of whatever happens to be illuminating it.

$$T_{SC} = \rho T_{ILLUMINATOR} \tag{2}$$

Combining the terms T_S and T_{SC} gives the effective radiometric temperature T_E of the object.

$$T_E = T_S + T_{SC} = \varepsilon T_O + \rho T_{ILLUMINATOR} \tag{3}$$

In outdoor imaging, the primary source of illumination is the down-welling of radiation from the sky itself. When a radiometer (an instrument for detecting thermal radiation) is aimed at the zenith, the radiometer will detect not only the residual radiation from deep space, but the low level of radiation that down-wells from the atmosphere itself, yielding a measured brightness temperature on the order of only ~60 K at 94 GHz [2]. Thus, a metal object with $\varepsilon = 0$ and $\rho = 1$ will have $T_E \sim 60$ K, and will, thus, appear very cold in an image. Imaging can be accomplished by measuring T_E as a function of position in the scene, thus creating a two-dimensional (2-D) map or image of the scene. Note that the above is highly simplified, not taking into account such factors as viewing angles, surface orientation, polarization effects, variations in the sky temperature as a function of angle relative to zenith, and both atmospheric emissions and attenuation along the line of sight of the measurement. Such factors have been accurately modeled in simulations [5].

Imaging Principles

The observed radiometric temperature of a scene is based on the following factors: emissions from scene constituents, reflections of the down-welling sky radiation by the scene, up-welling atmospheric emissions between the scene and the observer, and propagation of electromagnetic energy from the scene to the observer. Figure

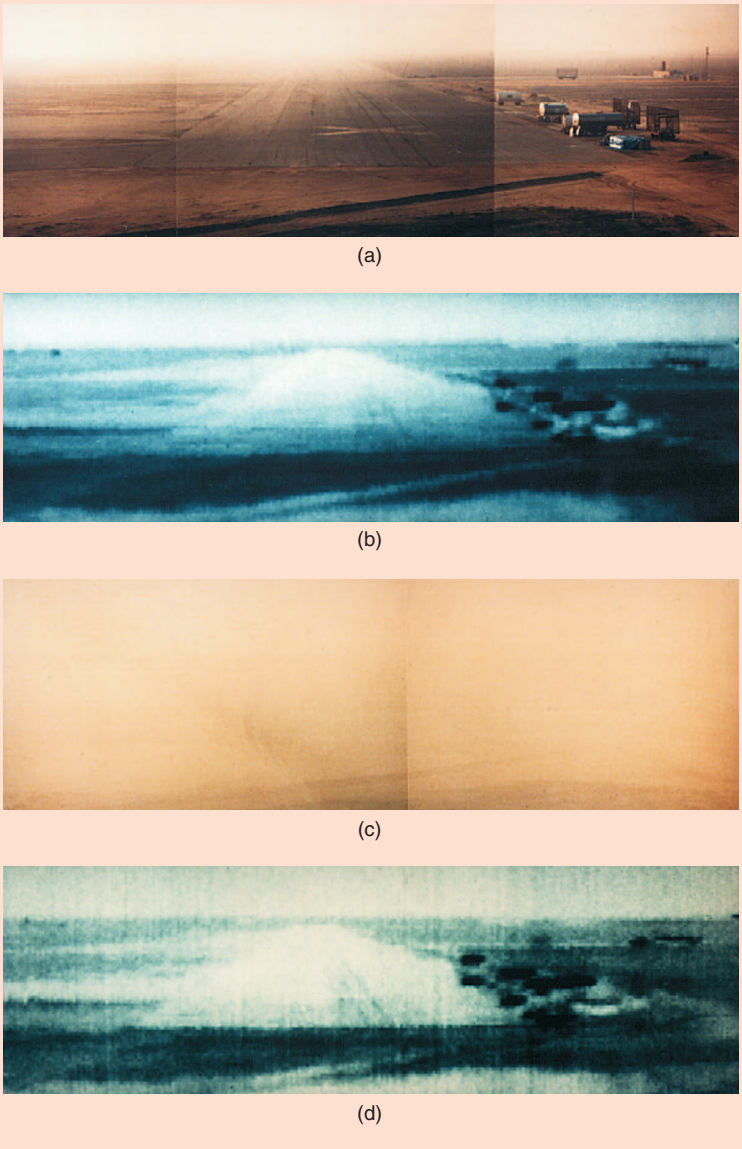


Figure 4. *PMMW images of a runway viewed from the glide slope before touchdown: (a) and (c) show visible images in clear and foggy weather; (b) and (d) show the corresponding PMMW images.*

Authorized licensed use limited to: Katholieke Universiteit Leuven. Downloaded on July 02,2010 at 06:43:35 UTC from IEEE Xplore. Restrictions apply.

3 illustrates these scene constituents. Image contrast is provided by differences in material, temperature, and sky illumination of the scene. Sky illumination is typically low level, i.e., radiometrically cold, at the zenith, rising to ambient temperatures at the horizon. Notice that the sun's illumination is not needed to generate a millimeter-wave radiometric temperature-based image of the scene.

An example of a radiometric image is illustrated in Figure 4. This figure contains a series of images that were obtained with a single 94-GHz radiometer mounted at the focus of a scanning 48-in diameter Cassegrain dish antenna. These images, acquired in both clear (b) and foggy (near zero visibility) weather conditions (d), are of a runway as it would look to a pilot just before touchdown. Visible images (a) and (c) are included for comparison. The scanning process involved the repeated tilting of the dish antenna aim point up and down while slowly panning the entire dish assembly from left to right. In this manner, the footprint of the antenna pattern on the scene was slowly moved over the entire scene. In this radiometric (or PMMW) image, the increasingly darker shades denote increasingly colder radiometric temperatures, although this can be reversed for aesthetic or other reasons. The equipment parked next to the runway appears cold because their metal surfaces, which are nearly fully reflective, reflect the cold overhead sky. The asphalt runway, a good reflector at grazing incidence, reflects the sky at the horizon, which is warmer than the overhead sky. The dirt adjacent to the runway is colder than the asphalt because the roughness of the dirt surface mixes the reflections from various parts of the sky, effectively lowering the dirt's radiometric temperature.

The important features to notice in Figure 4 are the images through fog. The visual images are totally obscured except for the near foreground, while the PMMW images are nearly unaffected by the fog. An interesting feature that emerges from the PMMW images is the mirror reflection of the parked equipment on the asphalt runway. This occurs because the asphalt runway, instead of reflecting the warm sky at the horizon, now sees a colder part of sky overhead via reflections off the equipment. Note that PMMW images, unlike radar images, have a visual quality, but with less resolution than a visible light picture.

The limitation of PMMW imaging is that image resolution, i.e., sharpness, is degraded compared to visible and IR images. The lower resolution is a consequence of the longer wavelengths used relative to the aperture size of the sensor's collection optics. Resolution improves with increases in the aperture size. This is illustrated in Figure 5 at 94 GHz (3.1 mm wavelength) for three different dish antenna aperture sizes. As can be seen, the image becomes sharper as the aperture diameter increases. The same effect can also be attained with a higher frequency (shorter wavelength).

The limits on the resolution, however, will always limit the range over which imaging can be performed, and can be more restrictive than the atmospheric propagation constraints. For example, In Figure 5(b), just to the right of the large black bar in the upper left of the image, a large metal hangar building, are three black spots. These are school buses at a range of 3,570 ft. These spots blur out to near nonexistence in Figure 5(d). Thus, the challenge is to construct a sensor that has a high enough frequency that is small enough to fit easily within an aircraft platform, for example, and yet still provide sufficient resolution to permit safe and accurate navigation, landing, surveillance, or other desired functions.

With the advent of the PMMW video camera and the ability to view the world in the millimeter-wave regime, low-visibility conditions as a threat to safety or a hindrance to travel will be overcome.

The PMMW Camera

PMMW Imaging

As previously stated, all objects radiate or reflect natural radiation across the frequency spectrum. Similar to

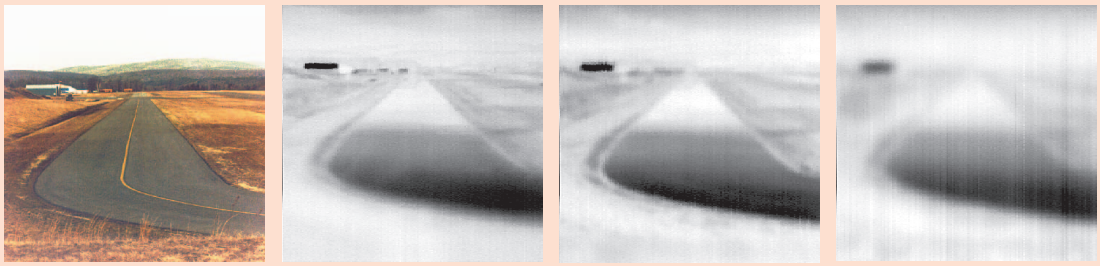


Figure 5. *The airport scene in visible light (a) with varying aperture sizes for the 94-GHz PMMW scanning system: (b) 48, (c) 24, and (d) 12 in.*

Authorized licensed use limited to: Katholieke Universiteit Leuven. Downloaded on July 02,2010 at 06:43:35 UTC from IEEE Xplore. Restrictions apply.

a visible camera (which detects visible radiation) and an IR camera (which detects IR radiation), a PMMW camera detects millimeter-wave radiation from the scene. All cameras are composed of a means to measure the radiation level from the scene and a means for forming the image (directing the radiation onto the measurement means). The following will briefly describe these means for the millimeter-wave regime, and will, for the most part, be recognized as extensions of what is done in the microwave regime.

The measurement of the scene radiation can be performed by a variety of methods. A typical method utilizes radiometers, which are basically calibrated receivers of thermal radiation. Radiometers come in several configurations, but the two most prevalent are the total power and the Dicke radiometers [6]. As the name implies, the total power radiometer simply integrates the power the receiver collects and provides a measurement of the total power collected. Likewise, the Dicke radiometer collects the scene radiation, but for only half the time. During the other half, it views a reference load, and by rapidly switching between the two sources of radiation, it obtains a measurement of the received power level that is less sensitive to instrumental drifts. The receiver itself, whether configured as a total power or Dicke radiometer, can be built in many ways. The simplest is the bolometer, in which the incident radiation is focused onto a detector element, causing a temperature rise that is used to infer the incident power level. Somewhat more complex are electronic means that directly amplify the incident radiation and measure the power content of the resultant signal using a square-law detector. Finally, there are receiver designs that utilize both the amplitude and phase information of the incoming radiation. This article will deal primarily with total power or Dicke radiometer configurations using electronic amplification of the incoming signal.

There are also many means for forming the image. As described earlier, a single focused receiver can be raster scanned across the scene to form the image. The manner in which the radiation is focused onto the receiver varies from system to system, ranging from dish antennas as used by radio astronomers, to the quasi-optical use of plastic lenses having the proper dielectric constants. Systems have also been designed and built to scan a small array of focused receivers using mechanical methods (spinning mirrors or antennas, rotating arrays, etc.) Others scan a line array of focused receivers through the simple motion of an aircraft, a so-called "pushbroom" configuration in which the footprint of the array of receivers on the ground is swept along by the aircraft movement. Such a pushbroom camera was built by NGST for the Office of Naval Research and was used to create the 180° × 30° panoramic picture in Figure 6. Here the line array was mounted vertically and the camera was rotated about a vertical axis to form the image. The most sophisticated methods involve the electronic scanning of the antenna pattern across the scene through phased-array techniques and interferometric methods using sparse arrays of widely separated antennas as performed in radio astronomy and other surveillance systems. Research groups around the world in academia, industry, and government have utilized these and other very novel and innovative methods to form PMMW images. This article will not review these many approaches, but the reader is referred to the suggested list of reading materials at the end of this article.

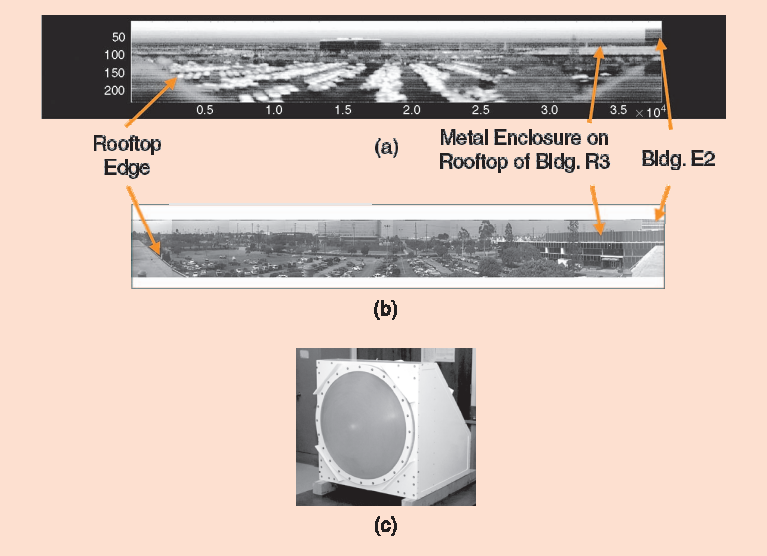


Figure 6. *Panorama view from the rooftop of a building, overlooking a parking lot and other structures. The PMMW image (a) was taken with (c) and covers a 180° horizontal and 30° vertical view. White is cold in this image. The visible-light image (b) is a collage of video camera image frames.*

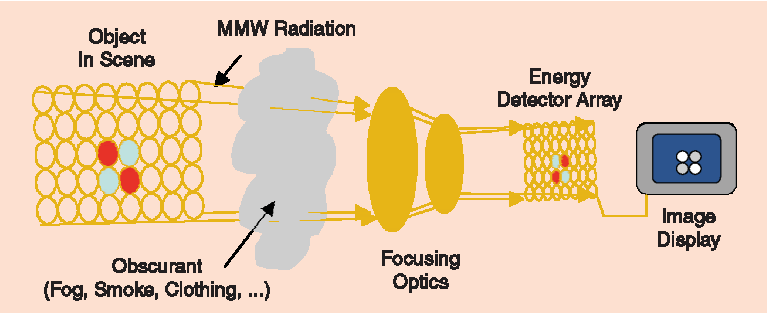


Figure 7. *PMMW imaging is similar to visible-light video camera imaging.*

Authorized licensed use limited to: Katholieke Universiteit Leuven. Downloaded on July 02,2010 at 06:43:35 UTC from IEEE Xplore. Restrictions apply.

In order to generate a video-like, real-time sequence of PMMW images, several methods have been investigated and developed around the world. These range from the rapid mechanical scanning of a small array, which has been shown to yield video-like PMMW imagery, to the complex but innovative phased-array approach utilizing the frequency regime to perform the required rapid scanning [7], [8]. A third approach uses a configuration similar to what is commonly used in visible and IR video cameras, that is, the use of a 2-D array of detectors. NGST has taken this approach in its development of PMMW imaging technology, taking advantage of the receiver technology it has developed, basically a complete radiometer on a chip.

As depicted in the sketch of Figure 7, the millimeter-wave radiation from the objects within a scene is focused onto a focal-plane array (FPA) of millimeter- wave receivers. By measuring and recording the variation in the resultant detected power or intensity levels across the scene, sequences of scene images can be collected and displayed to form a video-rate image stream.

PMMW Camera

Several recent technological advances have enabled the exploitation of millimeter waves. The advent of millimeter-wave monolithic integrated circuit (MMIC) technology has greatly increased the regime's potential; direct, low-noise amplification, and detection of millimeter-wave radiation are now a reality. Low-noise amplifiers utilizing pseudomorphic high electron mobility transistor (PHEMT) technology on gallium arsenide (GaAs) substrates were first developed, then later combined with on-chip switches and a sensitive detector diode, to form a complete MMIC-based, 89-GHz Dicke-like receiver on a single 2 × 7-mm chip having a noise figure of ~5.5 dB and bandwidth of 10 GHz [9]-[12]. The combination of high-sensitivity, low-cost, and low-power operation afforded by this MMIC device has enabled the construction of the world's first FPA PMMW video camera, shown in Figure 8 [13]-[15]. The MMIC chip is shown in the upper left, and four of them are placed on a 1 × 4 module to form a building-block unit for the camera FPA. The full FPA contains 260 of these 1 × 4 Modules (1,040 receivers), arranged in 26 planar cards of 40 receivers each. It operates according to the concept outlined in Figure 7.

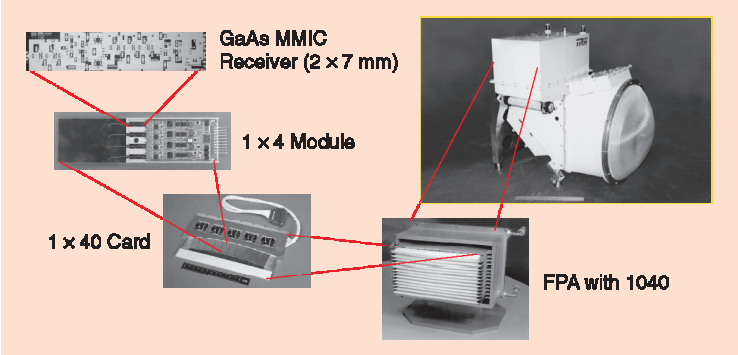


Figure 8. *The NGST PMMW video camera, shown here with its FPA components, was designed, built, and flight tested (from 1994-1999) by a consortium led by NGST, with participation by Boeing, Honeywell, and Composite Optics, Inc. under a White House Joint Dual-Use Technology Project. This project was cofunded by the Defense Advanced Research Projects Agency and managed by the National Aeronautics and Space Administration-Langley Research Center.*

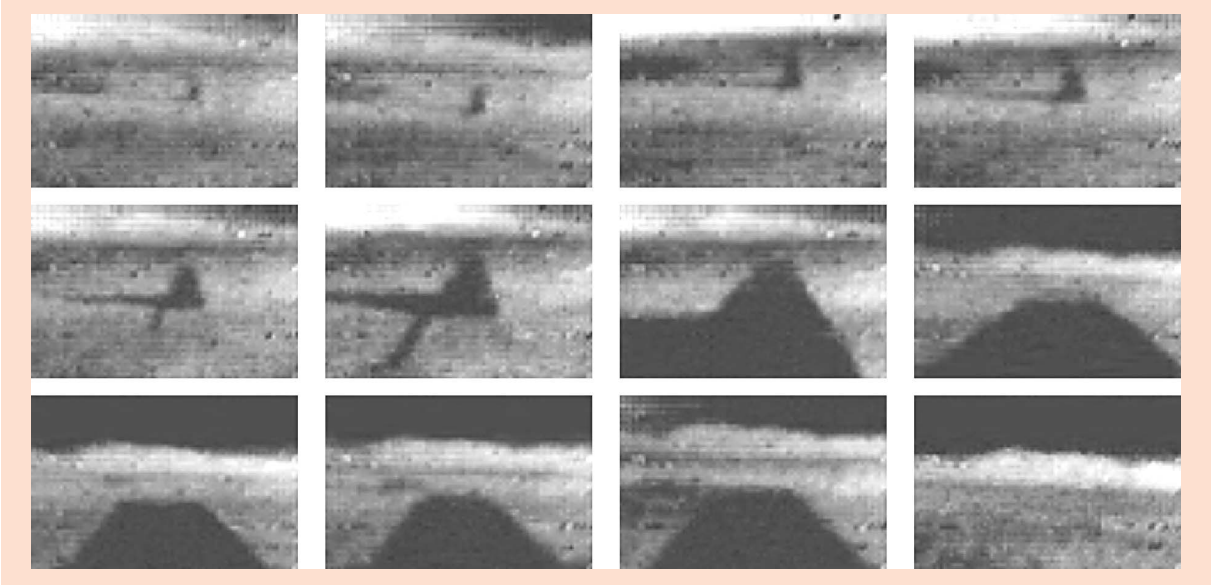


Figure 9. *Sequence of images (6-s intervals) taken with the PMMW video camera mounted on an aircraft of a dirt-over-dirt runway approach and fly-over.*

Authorized licensed use limited to: Katholieke Universiteit Leuven. Downloaded on July 02,2010 at 06:43:35 UTC from IEEE Xplore. Restrictions apply.

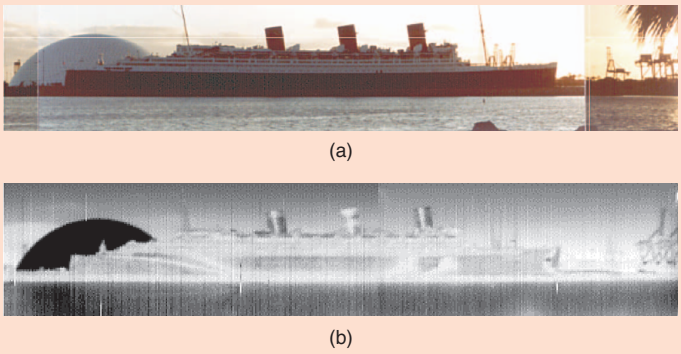


Figure 10. *(a) Visible and (b) PMMW images of the Queen Mary and former Spruce Goose dome in Long Beach, California, harbor. The ship is 1,700 ft from the imaging system; black represents cold.*

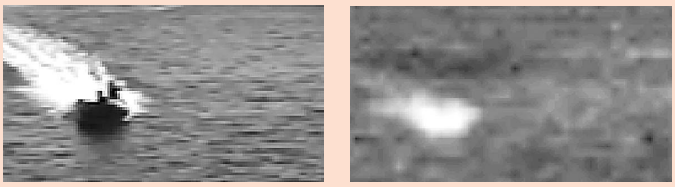


Figure 11. *(a) Visible and (b) PMMW images of a Zodiac inflatable and its wake.*

The PMMW video camera shown in Figure 8 uses an 18-in diameter plastic lens to collect and focus the radiation (a secondary lens within the camera is not visible), yielding a diffraction-limited 0.5° angular resolution. The size of the array, coupled with the optics, yields a 15° horizontal × 10° vertical field of view. A 45° turning mirror directs the focused radiation onto the FPA. This mirror also serves to dither the image on the FPA, i.e., it moves the image to four locations at the corners of a 0.5 × 0.5-pixel square, thereby quadrupling the number of points and attaining Nyquist sampling of the scene. The camera is capable of an image update rate of 17 Hz (with a display rate of 30 Hz), with a minimum resolvable temperature of ~2 K [16].

The PMMW video camera was successfully tested on the ground, in flight, and at sea [17]. Flight testing began in September 1997 aboard a U.S. Air Force KC-135 that was flown into numerous airports for runway approach imaging. Under contract with the Office of Naval Research, the PMMW video camera was also flown on a UH-1N helicopter and a Twin Otter aircraft along the coast between Los Angeles and San Diego, California. Video-rate image sequences were collected from altitudes ranging from 500 to 5,000 ft in both clear and overcast conditions.

Applications

As clearly indicated in the following, PMMW imaging sensors are useful for a wide variety of commercial and military missions requiring near-all-weather operations, as well as covertness (since there are no camera emissions). In addition, high sensitivity to metal objects, man-made targets, and ship wakes, as well as reduced sensitivity to variations in clutter, make a PMMW video camera an effective sensor asset. All of the images were taken either with the NGST PMMW video camera (single frames or sequences of single frames from the video sequence can only be shown here) or with a single raster-scanned 94-GHz radiometer mounted on a dish antenna, both described earlier in this article.

Aircraft Landing and Guidance

Covert, autonomous landing and taxiing in fog or smoke by helicopters and other aircraft is a mission of major relevance to both military and commercial operations. Figure 9 shows a sequence of images (6-s intervals, or every hundredth frame) taken from a PMMW video showing an approach to a dirt-over-dirt runway in the California desert in February 1999. The sequence starts at a distance of 1.7 nm from the runway threshold. The mountain range is approximately 12 nm away. The pilot relied only on this view, shown on a heads-up display along with an altimeter readout, and was able to fly the length of the runway at an altitude of 50 ft. Note that white is colder in these images. The smoother runway reflects the sky at the horizon, thus appearing warmer.

Low-Visibility Navigation and Situational Awareness

A PMMW imaging system can be employed on patrol boats and amphibious landing vehicles (LCACs) as well as other ground and seagoing vehicles to provide covert, near-all-weather visibility for navigation, target location, and other enhanced vision needs, especially in fog and through marine cloud layers. Figure 10 shows a raster-scanned image (using a single 94-GHz radiometer at the focus of a 48-in aperture dish antenna) of a harbor scene in Long Beach, California, one that would not have been impeded by fog if it had been present. Note the metal-domed structure reflecting the cold sky.

Perimeter Surveillance

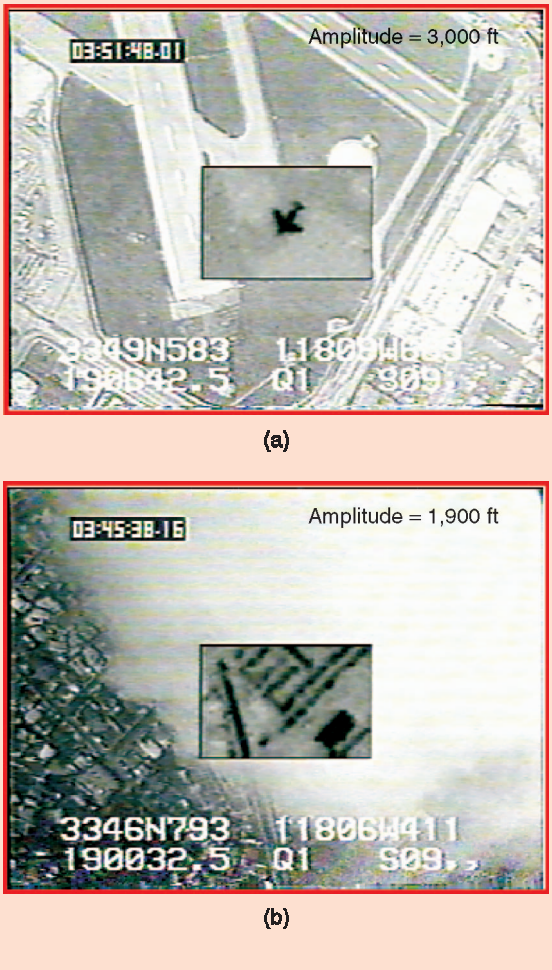
Near-all-weather surveillance of harbors, docks, and other designated areas can be performed with PMMW sensors. In addition, monitoring of all traffic into and out of specified areas is easily accomplished. In Figure 11, a small rubber inflatable and its wake (which appears warm) are readily detected by the PMMW video camera from the deck of a PC boat at a range of 300 ft.

Authorized licensed use limited to: Katholieke Universiteit Leuven. Downloaded on July 02,2010 at 06:43:35 UTC from IEEE Xplore. Restrictions apply.

Figure 11(a) is from a visible-light video camera, and Figure 11(b) is a still frame from the PMMW video camera, with white showing warmer areas. This type of target is not easily detected by radar.

Reconnaissance and Surveillance

An aircraft or unmanned aerial vehicle equipped with a PMMW camera can be used for near-all-weather look-down reconnaissance missions like the detection of ship wakes, low-radar cross-section boats, critical mobile, or other targets. In Figure 12, a single frame from a sequence taken by the PMMW video camera mounted on a Twin Otter, is superimposed on the corresponding visible-light still from a coboresighted video camera. In Figure 12(a), a C-17 is resolved from an altitude of 3,000 ft. The PMMW signature of metal targets is unique in the PMMW frequency regime, thus permitting auto-detection of such targets, as is evident in Figure 12, where black shows colder objects. The image on the right is of roadways and buildings imaged through a cloud bank, from an altitude of 1,900 ft.



(a)

(b)

Figure 12. *(a) PMMW imagery superimposed on a visible-light still frame of a C-17 on a taxiway and (b)PMMW image of roadways and buildings through clouds.*

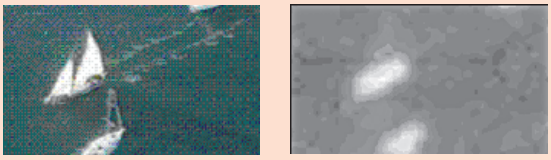
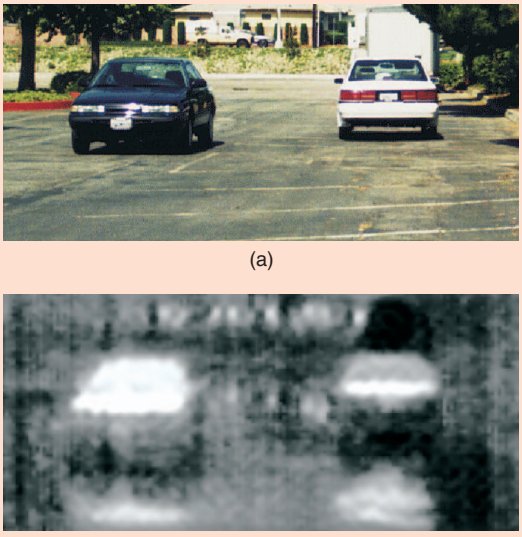


Figure 13. *(a) Visible-light and (b) PMMW images of sailboats.*



(a)

(b)

Figure 14. *(a) Visible-light and (b) PMMW images of two automobiles taken at ground level (white is cold in this image.)*

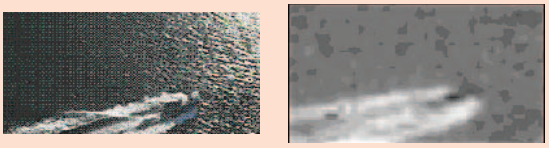


Figure 15. *(a) Visible-light and (b) PMMW images of a small metallic ship and its much larger warm-appearing wake.*



Figure 16. *PMMW imagery superimposed on a visible-light still frame of a PMMW beacon (which is undetectable in visible light) that clearly stands out in the PMMW image through a cloud.*

Authorized licensed use limited to: Katholieke Universiteit Leuven. Downloaded on July 02,2010 at 06:43:35 UTC from IEEE Xplore. Restrictions apply.

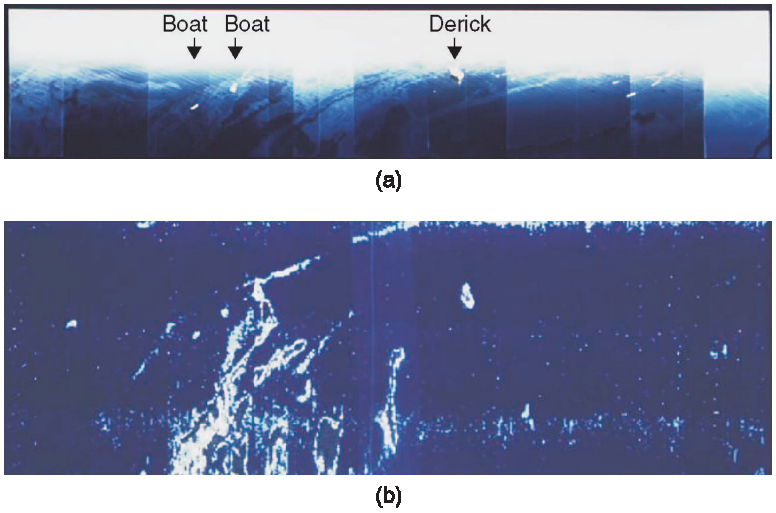


Figure 17. *(a) Visible and 94-GHz (b) PMMW image of an oil spill off of Huntington Beach, California, in 1990.*

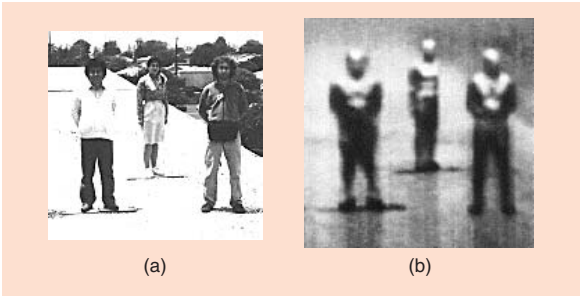


Figure 18. *(a) Visible image and (b) PMMW image of three people standing in the open outdoors. White represents cold.*

Search and Rescue

PMMW images can be used for search and rescue or reconnaissance under low-visibility conditions. Figure 13 shows several small fiberglass/wood sailboats visible on the water from an altitude of 350 ft and a range of 500 ft. Figure 13(a) is from a visible-light video camera, and Figure 13(b) is from the PMMW video camera, with warm shown as white.

Ground Navigation

Armored vehicles moving in fog, smoke, or sandstorms can benefit from a camera that presents a forward view essentially unaffected by those conditions, as an example but with no obscurant. Figure 14 shows two automobiles imaged at ground level using a single 94-GHz radiometer mounted on a scanning 24-in dish antenna and adjusted to focus at approximately 50 ft.

Drug Interdiction

PMMW imaging easily detects small boats and their much larger wakes against water. This capability can greatly aid in the detection and capture of drug traffickers. The long, trailing wakes of boats clearly stand out against the water and can be used to trace back towards their point of origin. Figure 15 depicts both a visible and a PMMW video camera still frame image of a small metallic boat and its long trailing wake. Such an image would be obtained even with fog or a marine layer between the boat and the sensor.

Beacon Detection

Millimeter-wave beacons can extend the utility of the PMMW camera for beacon-aided search and rescue as well as locating beachheads, way stations, and drop, retrieve, and rendezvous zones. In Figure 16, a very low-power beacon is detectable from an altitude of 5,000 ft. Again, a single frame from a sequence taken by the PMMW video camera mounted on a Twin Otter is superimposed on the corresponding visible-light still from a video camera, clearly showing the beacon visible through the clouds.

Oil-Spill Detection

Oil on water will produce a detectable change in the observed radiometric temperature in the millimeter-wave regime through an interference effect similar to the way antireflection coatings on lenses work. In the case of millimeter waves, the oil layer can increase or reduce the radiometric temperature of the areas where the oil patches are by varying the effective emissivity of those areas through changes in thickness. The observed temperature can, in fact, be used to infer the thickness of the oil. The ability to detect oil on water using PMMW imaging techniques was demonstrated in 1990 during an oil spill off of Huntington Beach, California. A single scanning 94-GHz radiometer was flown over the spill in a helicopter and generated the image shown in Figure 17. The scanning was done with a spinning mirror (the vertical axis of the image starts at 10° from nadir and goes upwards ~60°. The PMMW image displays radiometrically warm areas as white, and these areas correspond to the oil on the water surface. The dark background corresponds to open water that is clear of oil. Distortions inherent between the scanned image and the montage of visible wide-angle lens pictures have not been corrected.

Imaging of People and Concealed Weapons Detection

The imaging of people in the millimeter-wave regime produces images that are somewhat eerie, especially when done outdoors. Millimeter waves can easily pen-

Authorized licensed use limited to: Katholieke Universiteit Leuven. Downloaded on July 02,2010 at 06:43:35 UTC from IEEE Xplore. Restrictions apply.

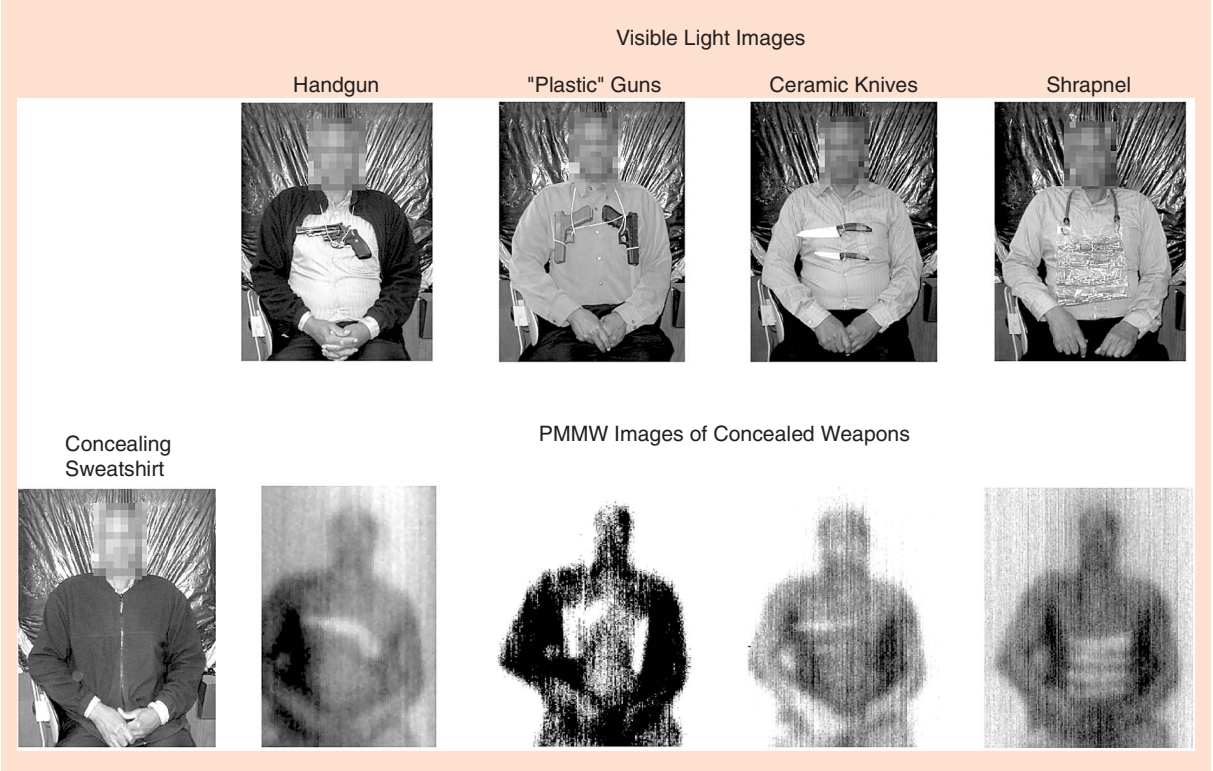


Figure 19. *Visible (top row) and corresponding PMMW images of an individual with various weapons concealed by the sweatshirt shown in the visible picture at the start of the bottom row. The PMMW images were acquired indoors with a 94-GHz radiometer on a scanning 24-in dish antenna. White is cold in these images.*

etrate clothing and hair. An image of a person will reveal a mannequin-like figure. The detected millimeter-wave radiation is a combination of the natural emissions from the body and, since skin has a reflectivity on the order of 10%, what is reflected from the surroundings. When outdoors, the sky is reflected off the skin of the upper surfaces of various body structures, while the warm ground is reflected from the lower body surfaces. This is illustrated in Figure 18, which was generated with a single 94-GHz radiometer mounted on a scanning 24-in dish antenna adjusted to focus at ~25 ft.

If an object is placed under the clothing that has a dielectric constant different than skin, the millimeter-wave image will reveal a radiometric temperature change caused by the object. For example, a metal gun hidden under the clothing will not only block the natural emissions from the body but will reflect the radiation from the surroundings. Even nonmetallic objects, such as plastics and ceramics, will have a similar effect.

If indoors, where the room is illuminating the body with radiation at ~295 K, the body's warmer emissions will be blocked or attenuated, and the object will be revealed to a PMMW imaging camera. Figure 19 is a collection of PMMW images of a person sitting indoors with various concealed weaponry. These were generated with a single 94-GHz radiometer on a scanning 24-in dish antenna and adjusted to focus at ~15 ft. In all of the images, the person was wearing a cotton sweatshirt to conceal the weapons. As can be seen, the metal handgun is clearly visible. The orange plastic handgun on the left is a training gun, while the other plastic handgun is a Glock with a metal barrel, and both are visible in the millimeter wave. The ceramic knives and the shrapnel in the plastic bag simulating a suicide bomber's weapon can also be seen.

Conclusion

PMMW imaging has a variety of applications that can be of great use to make life safer and provide the military with a key advantage under low-visibility conditions, such as in fog, clouds, smoke, or sandstorms. Some of these applications have been presented with sample imagery, but many others are being studied by investigators around the world. Particularly exciting has been the advancement of MMIC technology to allow the development of the video-rate PMMW camera, and some of the vast amount of imagery test data has been presented here as well. The near-all-weather operation holds the promise of providing an autonomous enhanced vision landing capability for commercial airlines, and the covert manner and the uniqueness of the PMMW signatures of targets of interest make this new

Authorized licensed use limited to: Katholieke Universiteit Leuven. Downloaded on July 02,2010 at 06:43:35 UTC from IEEE Xplore. Restrictions apply.

window in the electromagnetic spectrum an extremely promising one for all branches of the military. With the advent of the PMMW video camera and the ability to view the world in the millimeter-wave regime, low-visibility conditions as as a threat to safety or a hindrance to travel will be overcome.

Acknowledgments

The work described here was partially funded by NGST Industrial Research and Development funding, a White House Joint Dual-Use Technology Program cofunded by the Defense Advanced Research Projects Agency and managed for the government by the National Aeronautics and Space Administration, Langley Research Center, under Cooperative Agreement NCCI-196, and the Office of Naval Research under contract N00014-96-C-0431 under the technical direction of Dr. William Miceli and Dr. Michael Pollock. The work presented in this article is the result of contributions from many people, and the authors wish to thank all of them, including Hiroshi Agravante, Barry Allen, Mike Biedenbender, Ronson Chu, Giovanni DeAmici, Dave Dixon, G. Sam Dow, Martin Flannery, Steven Fornaca, Bruce Hauss, Talbot Jaeger, Ron Johnson, Karen Jordan, Mark Kolodner, Roger Kuroda, Paul Lee, Calvin Liang, Eric Lin, Dennis Lo, Karen Luebkemann, Ali Marashi, Michael Mussetto, Bill Quon, Arlen Rowe, Jim Rupert, Tom Samec, Barry Stark, Alex Valles, Khoi Vu, Karen Yokoyama, Marlowe White, and many others.

Suggested Reading

Proc. SPIE Conf. on Passive Millimeter-Wave Imaging Technology, 1997 to present.

F.T. Ulaby, R.K. Moore, and A.K. Fung, *Microwave Remote Sensing*. Reading, MA: Addison-Wesley, 1981.

J.C. Fisher, Ed., "Passive microwave observing from environmental satellites," NOAA, Washington, DC, Tech. Rep. NESDIS 35, 1987.

A.R. Thompson, J.R. Moran, and G.W. Swenson, Jr., *Interferometry and Synthesis in Radio Astronomy.* New York: Wiley, 1986.

References

[1] F.T. Ulaby and K.R. Carver, "Passive microwave radiometry," in *Manual of Remote Sensing*, R.N. Colwell, Ed. Falls Church, VA: American Society of Photogrammetry, 1983, ch. 11, pp. 475-516.

[2] P. Bhartia and I.J. Bahl, *Millimeter Wave Engineering and Applications.* New York: Wiley, 1984, pp. 660-671.

[3] D.D. King, "Passive detection," in *Radar Handbook*, M.I. Skolnik, Ed. New York: McGraw-Hill, 1970, ch. 39, pp. 39-1 to 39-36.

[4] J. Preissner, "The influence of the atmosphere on passive radiometric measurements," *Symp. Millimeter Submillimeter Wave Propag. Circuits: AGARD Conf. Proc.*, no. 245, pp. 48/1-48/13.

[5] B.I. Hauss, P.J. Moffa, W.G. Steele, H. Agravante, R. Davidheiser, T. Samec, and S.K. Young, "Advanced radiometric and interferometric millimeter-wave scene simulations," in *Proc. NATO Workshop on Military Applications of Millimeter Wave Imaging*, Hanscom Air Force Base, MA, 1992.

[6] N. Skou, *Microwave Radiometer Systems: Design and Analysis.* Norwood, MA: Artech House, 1989, pp. 7-19.

[7] R. Appleby, R.N. Anderton, S. Price, N.A. Salmon, G.N. Sinclair, J.R. Borrill, P.R. Coward, P. Papakosta, A.H. Lettington, and D.A. Robertson, "Compact real-time (video rate) passive millimetre-wave imager," *Proc. SPIE Conf. on Passive Millimeter-Wave Imaging Technology III*, 1999, vol. 3703, pp. 13-19.

[8] J. Lovberg, R. Chou, and C. Martin, "Real-time millimeter-wave imaging radiometer for avionic synthetic vision," *Proc. SPIE Conf. on Sensing, Imaging, and Vision for Control and Guidance of Aerospace Vechicles*, J.G. Verly and S.S. Welch, Ed, vol. 2220, pp. 234-244, 1994.

[9] T.N. Ton, B. Allen, H. Wang, G.S. Dow, E. Barnachea, and J. Berenz, "A W-band, high gain, low-noise amplifier using PHEMT MMIC," *IEEE Microwave Guided Wave Lett.*, vol. 2, pp. 63-64, Feb. 1992.

[10] G.S. Dow, T.N. Ton, H. Wang, D.C.W. Lo, W. Lam, B. Allen, K.L. Tan, and J. Berenz, "W-band MMIC direct detection receiver for passive imaging system," in *1993 IEEE MTT-S Int. Microwave Symp. Dig.*, p. 163.

[11] D.C.W. Lo, H. Wang. B. Allen, G. Dow, K. Chang, N. Biedenbender, R. Lai, S. Che, and N.D.Yng, "Novel monolithic multi-functional balanced switching low noise amplifier," *IEEE-Microwave Theory Tech.*, vol. 42, pp. 2629-2634, Dec. 1994.

[12] D.C.W. Lo, E.W. Lin, H. Wang, M. Biedenbender, R. Lai, G. Ng, G.S. Dow, B.R. Allen, "MMIC-based W-band Dicke switched direct detection receiver," in *IEEE 1995 GaAs IC Symp. Tech. Dig.*, pp 226-229.

[13] G.S. Dow, D.C.W. Lo, Y. Guo, E.W. Lin, T.T. Chung, M.D. Biedenbender, O. Miromontes, A. Marashi, L. Yujiri, P.S.C. Lee, M.M. Shoucri, and B.R. Allen, "Large scale W-band focal plane array for passive radiometric imaging," in *1996 IEEE MTT-S Int. Symp. Dig.*, vol. 1, pp. 369-372.

[14] R. Kuroda, G.S. Dow, Y. Guo, R. Johnson, M. Biedenbender, A. Marashi, L. Yujiri, and M. Shoucri, "Direct detection MMIC FPAs for MMW imaging," in *Proc. SPIE Conf. Passive Millimeter-Wave Imaging Technology*, Orlando, FL, 1997, vol. 3064, pp. 90-97.

[15] R.T. Kuroda, G.S. Dow, D. Moriarty, R. Johnson, A. Quil, S.D. Tran, V. Pajo, S. Fornaca, and L. Yujiri, "Large scale W-band focal plane array developments for passive millimeter wave imaging," in *Proc. SPIE Conf. on Passive Millimeter-Wave Imaging Technology II*, Orlando, FL, 1998, vol. 3378, pp. 57-62.

[16] L. Yujiri, H. Agravante, M. Biedenbender, G.S. Dow, M. Flannery, S. Fornaca, B. Hauss, R. Johnson, R. Kuroda, K. Jordan, P. Lee, D. Lo, B. Quon, A. Rowe, T. Samec, M. Shoucri, K. Yokoyama, and J. Yun, "Passive millimeter-wave camera," in *Proc. SPIE Conf. on Passive Millimeter-Wave Imaging Technology*, Orlando, FL, 1997, 3064, pp. 15-22.

[17] L. Yujiri, H. Agravante, S. Fornaca, B. Hauss, R. Johnson, R. Kuroda, B. Quon, A. Rowe, T. Samec, M. Shoucri, K. Yokoyama, "Passive millimeter wave video camera," in *Proc. SPIE Conf. on Passive Millimeter-Wave Imaging Technology II*, 1998, vol. 3378, pp. 14-19.

Authorized licensed use limited to: Katholieke Universiteit Leuven. Downloaded on July 02,2010 at 06:43:35 UTC from IEEE Xplore. Restrictions apply.